

Muon Track Reconstruction

Arohi Jain
 arohi91@yahoo.com
 Supervisor: Prof. Sudeshna Banerjee

Abstract : We have studied resistive plate chambers and scintillation detectors for detection of muon. In our project, we have experimentally observed and studied the V-I characteristics, voltage-efficiency characteristics and voltage-noise characteristics of an RPC. We have also used a prototype of ICAL detector with 12 RPC layers to observe muon tracks. Finally, we have made a routine to fit the muon tracks obtained from this data.

INTRODUCTION

A muon is one of the six subatomic particles that cannot be further subdivided into constituent particles, the other being electrons, tauons and neutrinos. The family of all these particles is called leptons. One common property of all leptons is their spin which is $\frac{1}{2}$ for all the four varieties. Thus they are all classified as fermions and obey the Pauli's Exclusion Principle. It is an unstable particle with a mean lifetime of $2.2 \mu\text{s}$. This comparatively long decay lifetime (the second longest known) is due to being mediated by the weak interaction.

Muons have a mass of $105.7 \text{ MeV}/c^2$, which is about 200 times the mass of an electron. Since the muon's interactions are very similar to those of the electron, a muon can be thought of as a much heavier version of the electron. Due to their greater mass, muons are not as sharply accelerated when they encounter electromagnetic fields, and do not emit as much bremsstrahlung (deceleration radiation). This allows muons of a given energy to penetrate far more deeply into matter than electrons, since the deceleration of electrons and muons is primarily due to energy loss by the bremsstrahlung mechanism. As an example, so-called "secondary muons", generated by cosmic rays hitting the atmosphere, can penetrate to the Earth's surface, and even into deep mines. Because muons have a very large mass and energy compared with the decay energy of radioactivity, they are never produced by radioactive decay.

Most muons come from cosmic rays. As they fall toward the earth, they ionize the atmosphere forming a shower of matter and anti-matter particles. These particles are known as pions (p) and are made up of up and down quarks and anti-quarks. They quickly decay into lighter things, such as leptons and electromagnetic radiation. This is where our muons come from: they are the results of an interaction between a proton and the atmosphere that produces a particle that decays into a muon, among other things. These showers are happening all the time. About 600 particles pass through your body each minute!

HOW TO DETECT A MUON

Cosmic rays, and muons in particular, are hard to detect because they are travelling very fast and pass through most materials without interacting. The trick to detecting them is to take advantage of the fact that they are charged particles. When a charged particle passes through a particular substance

it can ionize the surrounding particles and leave a trail. In our project here at TIFR, we use resistive plate chamber(RPC) and scintillation detection to detect muons. In RPCs, muons ionise the gas and hence they are detected. In scintillation detectors, muons excite the atoms/molecules that make up the scintillation detector causing a flash of light to be emitted. This light signal is then converted to photo-electrons which is then amplified to give strong electrical signals which are analyzed.

RESISTIVE PLATE CHAMBERS

An RPC(Fig. 1) is a particle detector utilising a constant and uniform electric field produced by two parallel electrode plates, atleast one of which is made of a material with high bulk resistivity such as glass - 10^{10} - 10^{12} Ωcm (or bakelite (phenol-formaldehyde polymer)). RPCs are simple to construct and operate, yet rugged, well adapted to inexpensive industrial production. The main features of these detectors are large signal output, excellent time as well as position resolutions and low cost per unit area of coverage.



Fig.1 Schematic of a Resistive Plate Chamber

A gas mixture (in our case - Freon 95.2%, Isobutane 4.5%, SF_6 0.3%) with a high absorption coefficient for ultraviolet light is flown through the gap(2 mm) between the electrodes. Freon absorbs the charged particles before any further avalanche is produced. R134a is used, since it is environment friendly. Isobutane, being an organic gas, is used to absorb photons from recombination process, limiting the formation of secondary avalanche from primary ionization. It is because of this property is known as Quenching Gas. SF_6 is used to trap the excess energetic electrons from the gas volume before they can initiate a new avalanche. The separation is ensured by poly-carbonate button spacers placed in a grid like pattern. The four sides of the gap are then sealed.

When the gas is ionised by a charged particle crossing the chamber, free charge carriers that are deposited in the gas gap trigger avalanches of electrons in the externally applied electric field and originate a discharge. Due to the high resistivity of the electrodes, the electric field is suddenly dropped down in a limited area($\sim 1\text{cm}^2$) around the point where the discharge occurred. Thus the discharge is prevented from propagating through the whole gas volume. The sensitivity of the counter remains unaffected outside this small area. On the other hand, due to the ultra-violet absorbing component of the gas mixture, the photons produced by the discharge are not allowed to propagate in the gas. This prevents secondary discharges from originating at other points of the detector. The propagation of the growing number of electrons induces a current on external strip electrodes.

The outer surfaces of the glass plates are coated with a conductive coating (of graphite). Graphite is used because it has high conductivity, chemical resistance and good mechanical properties.

Graphite forms no compounds due to corrosion, no protective surface films as do many metals. A high electric field of about 10kV is applied across these electrodes. Positive voltage is applied to one side and a roughly equal and negative voltage to the other side (for safety purposes). Two Mylar sheets of the same size and thickness 100 μm are placed just above this to provide better isolation. Pick up panels are placed over the Mylar sheet one set along X-direction another over Y-direction. The width of the pickup strip is 3 cm each.

There are two modes of operation for RPCs – Avalanche mode and streamer mode.

- Avalanche Mode: Ionized particles, created by primary ionization of gas through charged particles, are accelerated by the electric field and in their way to the electrodes they ionize the gas again to set in an Avalanche process. However this process stops as the internal opposite field is balanced by the external field and the charges are collected in the respective electrodes. The pulse height in this mode is of the order of few milli volts and amplifiers are required in this mode of operation. This mode is also called limited proportional mode.
- Streamer Mode: In this mode of operation, the electric field inside the gap is kept intense enough to generate limited discharges localized near the crossing point of the ionizing particle. Since this mode is operated at very high voltages, the secondary ionization continues until there is a breakdown of the gas and a continuous discharge takes place. The avalanche is followed by a streamer discharge & signal generated is large of the order few hundreds of milli volt. Hence no amplifiers are needed. Thus readout of Streamer mode RPCs is quite simple. However, this mode decreases the life of the detector severely, hence avalanche mode is preferred. The gas mixture has Freon: Argon: Isobutane in the ratio of 62:30:8 by volume in the streamer mode.

Iron calorimeter which is used to detect neutrinos is built layer by layer using low carbon steel plates with a RPC stacked between two steel plates. At TIFR, 2 ICAL prototype(Fig.2, Fig.3) are installed.



Fig.2 ICAL detector with 12 RPCs stack. Each RPC has an area of 2m x 2m with 64 pickup strips each for plane X and plane Y. This is installed in New INO Lab.

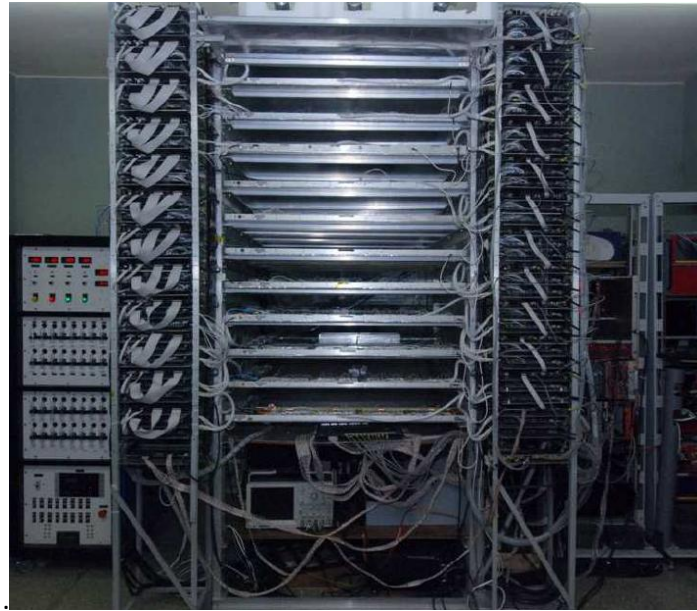


Fig.2 ICAL detector with 12 RPCs stack. Each RPC has an area of 1m^2 with 32 pickup strips each for plane X and plane Y. This is installed in room C127.

We have already discussed how RPC detects a muon. But in our study, we also use scintillator detectors as triggers along with RPCs.

SCINTILLATION DETECTORS

Scintillation detectors are made of materials which when struck by a particle or radiation, emit a flash of light i.e a scintillation. They are coupled to photomultiplier tubes to give electrical signals which can then be analyzed. A scintillation detector consists of scintillator, photomultiplier and light guide (may or may not be present). As the particle/radiation passes through the scintillator, it excites the atoms and molecules that make up the scintillator causing light to be emitted. This light is transmitted to the PMT either directly or through a light guide where it is converted into a weak current of photoelectrons which is then further amplified by an electron-multiplier system. In addition, wavelength shifting fibers may be used. These fibers absorb light from a range of wavelengths and emit light of a particular wavelength, which is more compatible with the PMT.

A good scintillator must be sensitive to energy (light output of a scintillator is directly proportional to the exciting energy), have a fast response time and a short decay time. It must efficiently convert exciting energy into fluorescent radiation and must be transparent to its fluorescent radiation so as to allow transmission of light. Emission in a spectral range should be consistent with the spectral response of the photomultipliers used. It should be able to distinguish between different types of particles based on the shape of the emitted light pulses, using the property that different fluorescence mechanisms are excited by particles of different ionizing power.

Light output response refers to the efficiency of converting ionization energy to photons. It determines the efficiency and resolution of the scintillator. The response of a scintillator is a function of the type of particle, its energy and also its specific ionization. It is also a function of temperature. This dependence is weak at room temperatures, but should be considered if temperatures very far from normal are to be considered.

PHOTOMULTIPLIER TUBES

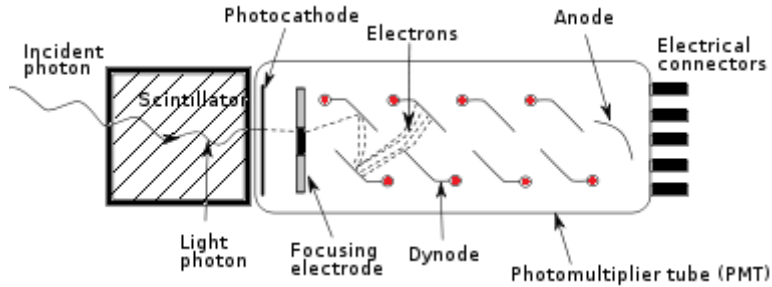


Fig.4 Schematic of a photomultiplier tube

They are electron tube devices that convert light into a measurable electric current. They are coupled to the scintillator to convert the the light into an electric signal. It consists of a cathode(a photosensitive material), electron multiplier section (or dynode string) and anode(signal collected here). A high voltage is applied to the cathode, dynodes, anode such that a potential ladder is set up along the length of the cathode-dynode-anode structure.

When an incident photon impinges upon the photocathode, an electron is emitted via the photoelectric effect. Because of the applied voltage, the electron is directed and accelerated towards the first dynode, where upon striking; it transfers some of its energy to the electrons in the dynode. This causes secondary electrons to be emitted, which in turn are accelerated towards the next dynode where more electrons are released and further accelerated. An electron cascade is thus created. At the anode, this cascade is collected to give a current which can then be amplified and analyzed. When used with a scintillator, it is used in the pulsed mode. If the cathode and the dynode systems are considered to be linear, the current at the output of the PMT will be directly proportional to the number of incident photons. Hence it is capable of providing information about the particle's presence and also the energy deposited by it in the scintillator.

The efficiency of the photomultiplier must also be taken into account when considering the efficiency of the scintillation detector since they are coupled. The PMT typically has an efficiency of 30%.

SCINTILLATOR MOUNTING

In our project we have used plastic scintillator made of Polyvinyl Toluene. It is cheap, flexible and can be produced in various shapes and sizes. We made a scintillator which has area of 31 cm x 31 cm with 30 grooves each of thickness 5mm. Each of these grooves contains five optical fibres.

Scintillator was first grooved in the Mechanical workshop. Then it was cleaned properly with Alcohol (Propan-2-ol). 150 WDM fibers were cut, each about 50 cm long.

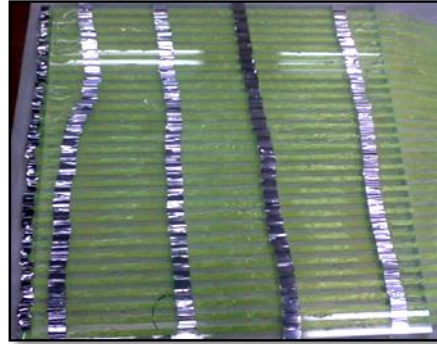


Fig. 5 Scintillator with glued fibers

Five of such fibres(Fig.5) were taken at a time and fitted in each of the grooves of the scintillator. They were fixed to the scintillator by means of Aluminium tape and glue. The glue used was E-30 CL Hysol. The glue was left to dry.



Fig. 6 Fiber ends in the cookie

One end of the fibres was inserted into an acrylic cookie(Fig. 6) and then glued to it and left to dry. Ends of scintillator and cookie containing loose ends of fibers were again polished(Fig. 7).

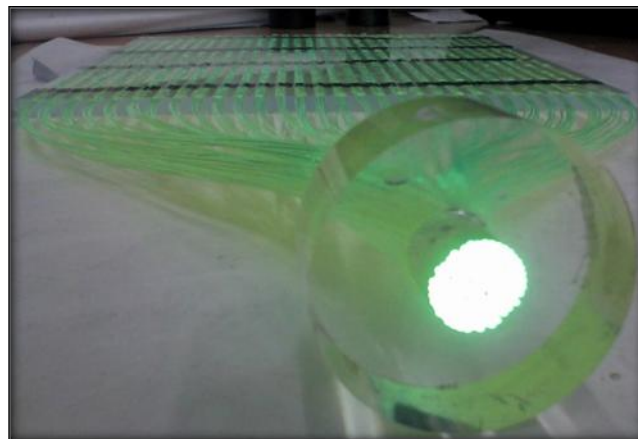


Fig. 7 Polished scintillator. We can see the bunch of fibers fitted in the cookie

An aluminium strip was fixed at one edge of the scintillator (the one away from the long end of the fibres). This serves as a good reflector. The scintillator was then covered in white "TYVEC" paper(Fig. 8).



Fig.8 Scintillator wrapped in TYVEC paper

Since the light is emitted isotropically by the scintillator, it must be reflected back to avoid losses. The Tyvec paper aids in this. The Tyvec paper was held in place by means of Aluminium tape and black tape. Next, it was covered with several layers of black Tedlar paper(Fig. 9). This was also fixed by means of black tape. The entire scintillator was covered extensively with black tape to avoid any external light from entering into it.



Fig. 9 Scintillator further wrapped in Tedlar sheet and then black tape

A photomultiplier tube was attached to the cookie which would collect the photons produced from scintillator. Hence, the scintillator was ready for use(Fig. 10).



Fig.10 Scintillator(31cm x 31 cm), 150 WLS fibers, with PMT

Precautions had to be taken so as not to break the fiber near the edges of scintillator and cookie. Also, PMT must not be exposed to light. PMT if exposed, will cause electrons to be produced and increase the dark current of PMT.

CHARACTERIZATION OF RPC:

My task was to characterise RPC AL03 being used in New Lab(Fig. 3).

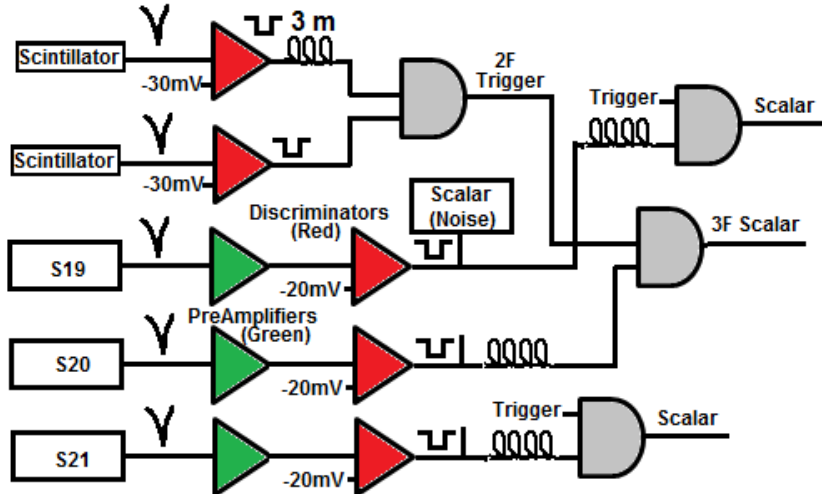


Fig . 11 Block Diagram of the trigger and signal generation. S19, S20, S21 are 3 strips of RPC AL03.

One scintillator each was placed above and below the RPC and it acted as a 2 fold trigger. The signal from each scintillator was sent to a discriminator (with a threshold of -30 mV) to convert the analog pulse into a NIM pulse. The outputs from one of the discriminators with delayed by 150 ns to avoid for jitters. The two outputs were then passed through an AND gate to get a trigger pulse (2F).

S20 was considered the main strip, S21 the right strip and S19 the left strip. The signal from RPC is weak and hence it is first amplified and then signal is obtained after passing through a Leading edge Discriminator(threshold -20mV). We then 'AND ' the signal from S20 with scintillator trigger to form a 3 fold signal. Efficiency of each strip is calculated by dividing the no. of signals in the 3 fold data by the no. of signals in the 2 fold data , both averaged over an interval.

$$\text{Efficiency} = 3F/2F *100$$

Similarly noise(in Hertz) can be calculated by averaging the noise collected in scalar over a time interval. In my experiment, I varied the voltage from 10.1kV to 9.2kV(decreased the voltage in steps of .1kV for a stable system) and obtained efficiency(Fig. 12) and noise(Fig. 13) for these voltages. I also obtained plots of noise(Fig. 14-16) over a period of time for these voltages. This data was taken from 18th – 20th June, 2012

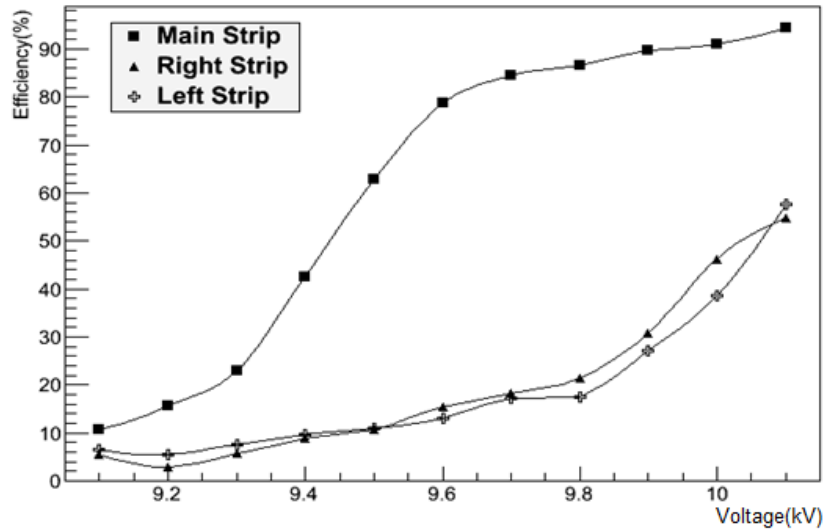


Fig. 12 Efficiency of RPC AL03 vs Voltage .

Graph(Fig. 12) shows the efficiency of the RPC -strip 20(main), strip 19 (right), strip 21(left) as a function of the high voltage applied. With increase in the high voltage applied, the efficiency for the RPC increases. However, there is a plateau region beyond 9.8kV which is optimum for the usage of the RPC, where the efficiency remains constant with increase in voltage.

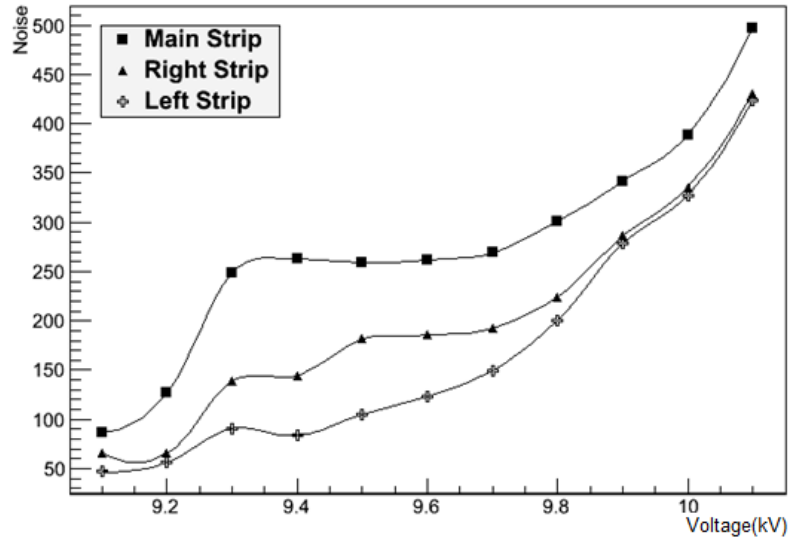


Fig. 13 Noise vs Voltage for RPC AL03 Strip 19, 20, 21

Graph(Fig. 13) shows the variation of noise in the RPC as the applied high voltage to the RPC is varied. As the high voltage increases, the noise rate also increases. The noise rate of the main strip is clearly more than the left and the right one.

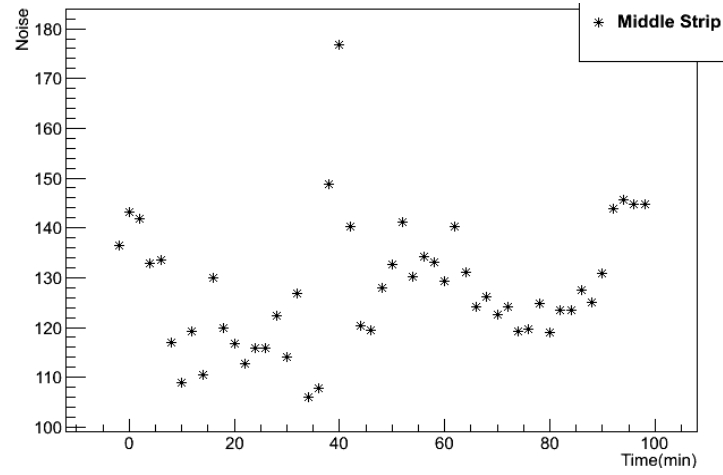


Fig. 14 Variation of Noise over time for voltage = 9.2kV

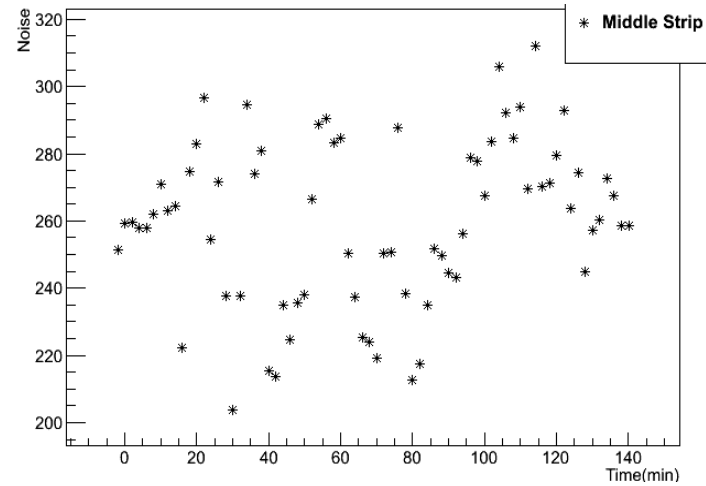


Fig. 15 Variation of Noise over time for voltage = 9.5kV

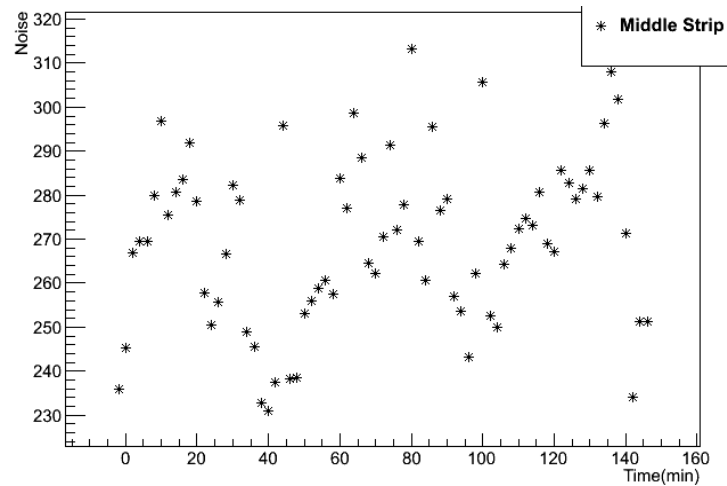


Fig. 16 Variation of Noise over time for voltage = 9.7kV

We observe that noise exhibits random fluctuations. The data for efficiency and noise rate of the RPC was taken twice. In the first attempt(15th – 18th June, 2012), the noise rate was exceptionally high, so the desired results were not obtained.

Along with this, I also did the **V-I characteristic** for the RPC AL03

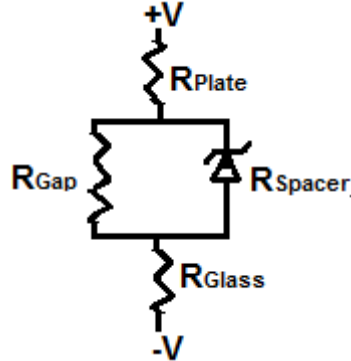


Fig 17. Circuit diagram for the glass RPCs

In the low voltage region, spacer resistance(Fig 17) is very high and therefore, gap spacer resistance is obtained while in the high voltage region, spacer resistance is zero, avalanche of electron - ion pair starts and break down occurs. This is the active region of RPC and the glass resistance dominates.

Equal and opposite voltages were applied at the two channels- A and B and the corresponding current values were observed. The current values were almost the same(Fig 18 & 19). Since the current is measured only at ends of the power supply, such a slight variation in the resistance values is admissible.

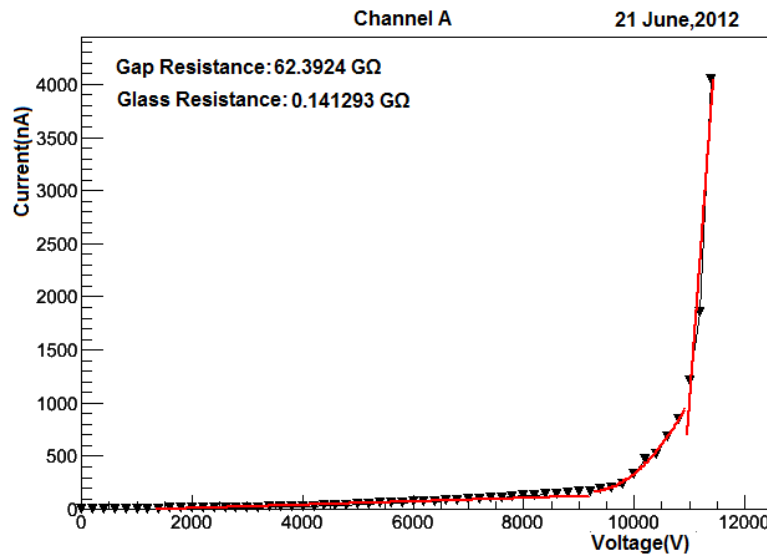


Fig 18. Channel A V-I characteristic curve

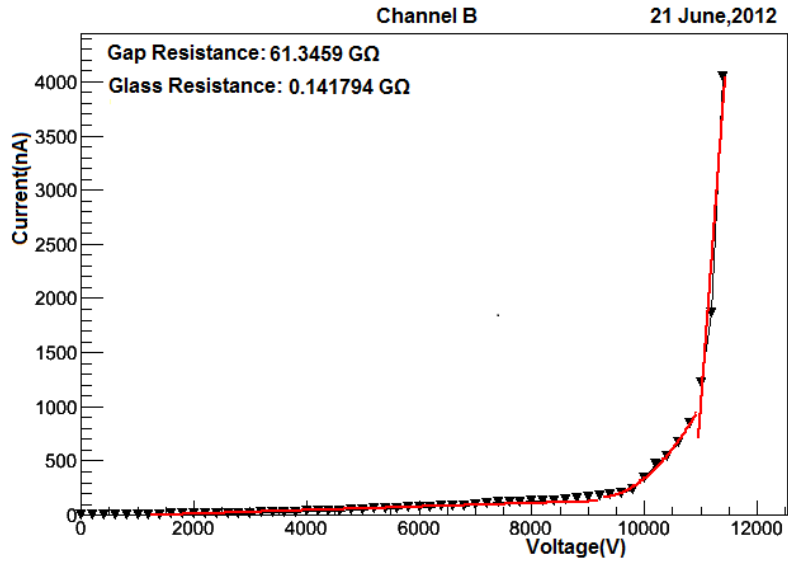
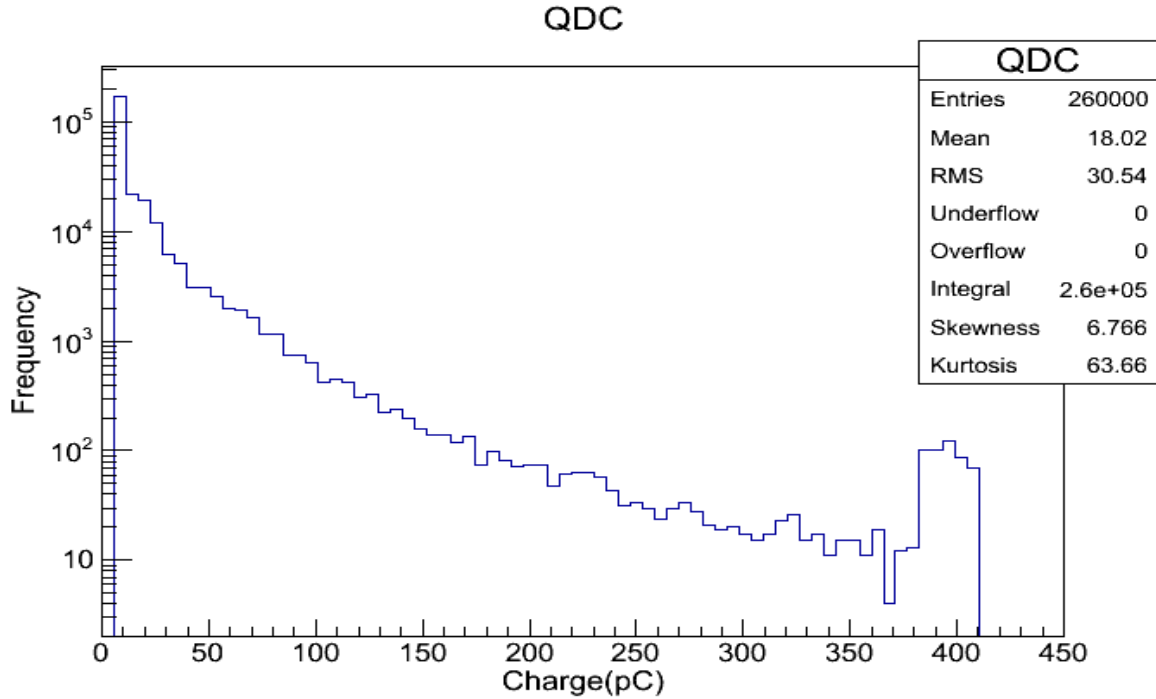


Fig 19. Channel B V-I characteristic curve

MUON TRACK DETECTION

Next, our task was to use these RPCs to track a muon. The experiment was performed at C130 lab which has 12 RPC layers. Two scintillator paddles, one each were placed on layer 1 and layer 11 to serve as a trigger for the passing muon. The paddle is 31 cm wide and placed at the center of RPC. RPC is 100cm wide so 2 pre-amplifier of the RPC on both the sides are disabled so that they do not give trigger. Biasing voltage for other pre-amplifiers was +6V and -6V. V was the output of the scintillator and T was the trigger of the RPC. Time lag may exist between these two because of the length of the path involved. In such cases, a cable for required length is introduced. A 2 metre cable provides a delay of 100ns. The data acquisition system takes 1s for the trigger.

We obtain the mean charge deposited on the scintillator. QDC gives data output in millivolts per count. We first plot the histogram of this voltage data and find the mean to be 180mV. The pedestal was set to 60 DAC counts and from the manual we know the value for $I_{pedestal}$ to be $1.94\mu\text{A}$. Corresponding to this, the offset in voltage was found to be 1.94mV. Hence, the net voltage will be voltage at any event – 1.94mV. From $q=CV$, and $C=100\text{pF}$, we can calculate the charge deposited as $(V-1.94)*0.1\text{picoCoulomb}$. For this charge data for scintillator, we obtain charge distribution histogram, which was fit with Landau distribution. It is observed that charge data obtained is a Landau distribution with a mean charge of about 5pC.

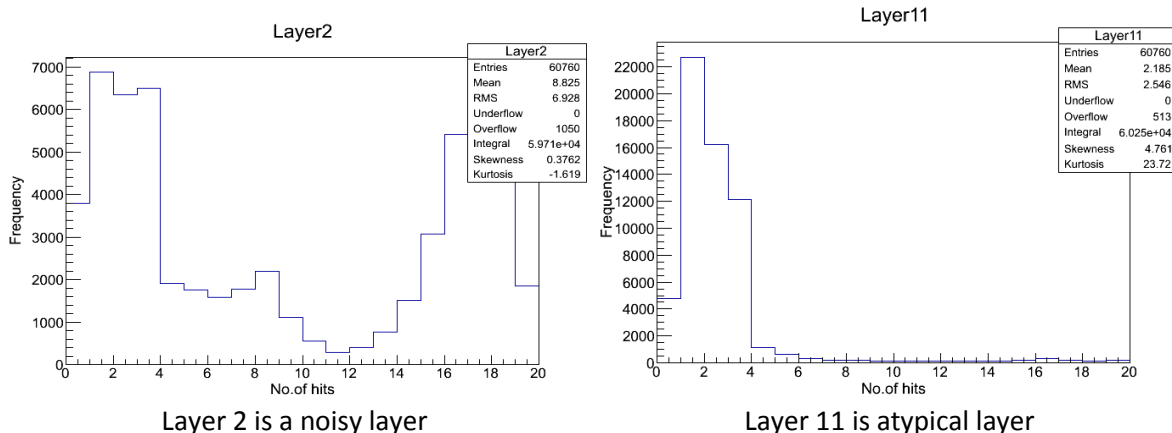


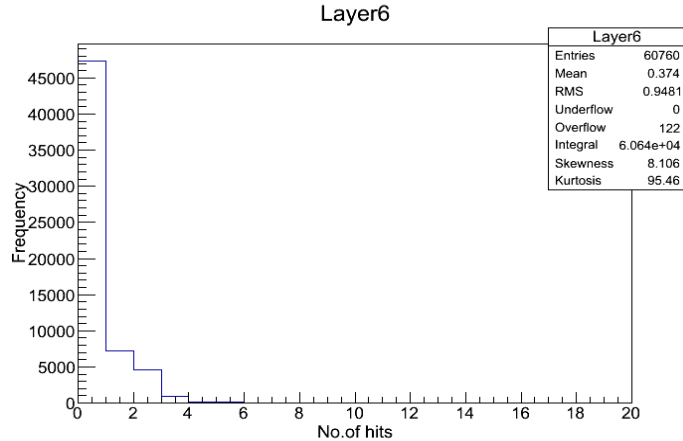
Charge distribution obtained from scintillator fitted with Landau distribution

Because the counter is of 12 bits, from 2 to $2^{12} = 4096$, so all the data greater than 4096 (due to noise or other disturbance), i.e., the overflow data is filled there. Hence we observe a small peak near 400pC. Also, as the pedestal is at 60 counts, so we do not see a clear distinction of pedestal from the charge peak obtained from scintillator data.

Hence, we started data analysis for the muon data collected from 12 RPCs. The data file obtained was a '.ine' file which was converted to txt file using using the TFile, TTree and TBranch classes. The text file contained the event number, layer number, strip number and the serial number (the number of times each layer is hit) and this .txt file was used for further analysis.

Plots for no. of hits in layer 2, layer 6 and layer 11 are displayed

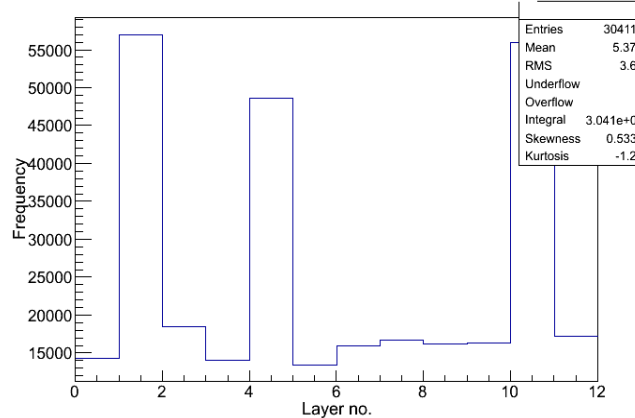




Layer 6 is a typical layer. All the layers that are not noisy show a similar pattern for the number of hits. As the layers 2, 4 and 10 show a much larger number of hits than the others, these are hence the noisy layers. Next we try to eliminate the layers with more than three hits (the noisy layers)

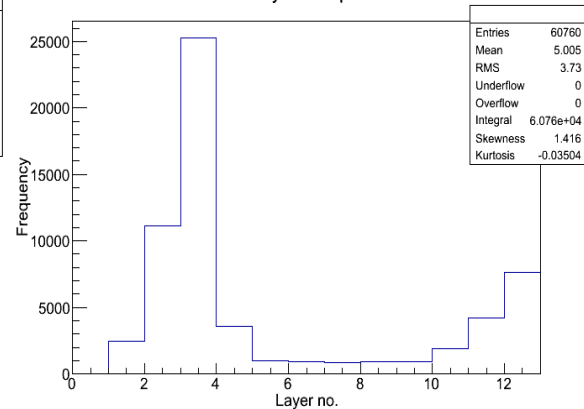
Plot for no. of times a layer has been hit

How many times a layer records hits



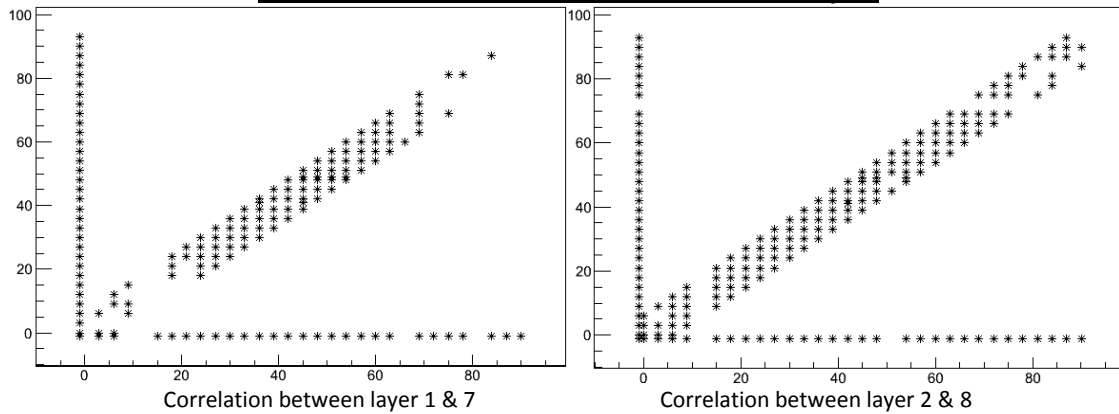
Plot for no. of layers have been hit per event

No. of Layers hit per event

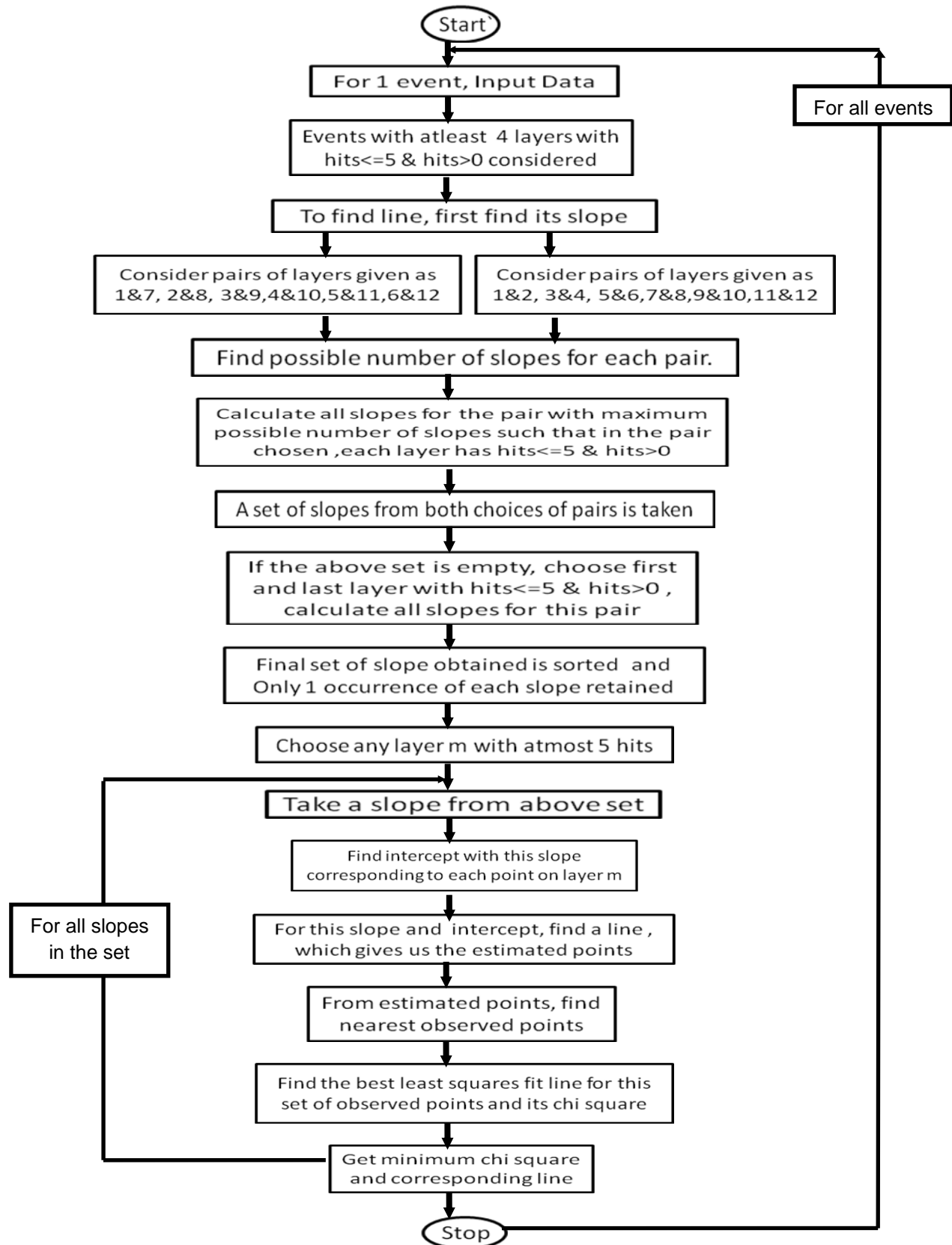


This shows no of layers hit per event. We see that about 38000 events have almost 3 layers with hits. Very few events have all the layers hit, these are the ones that correspond to the muons. A lot of them have few layers being hit. This is either due to electronic noise or something to do with the pre-amplifiers. Only such events which have atleast 4 layers with hits would be considered for reconstruction of the muon tracks.

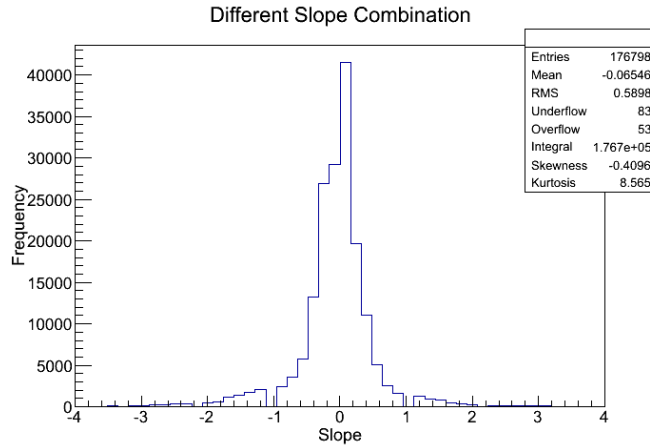
Plot for correlation in hits between different layers



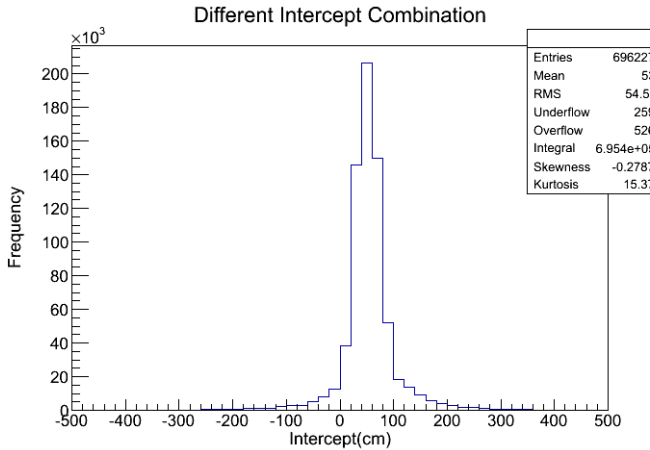
In the following page we discuss the algorithm for reconstruction of muon tracks.



Plot for slopes and intercept obtained before best chi line is chosen

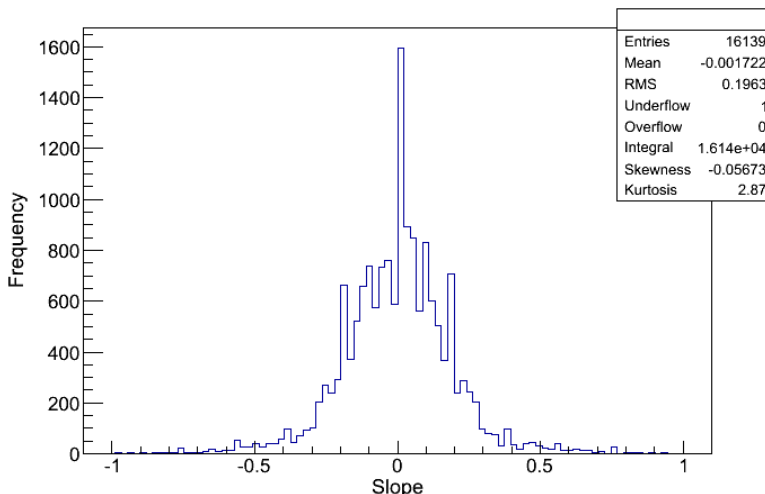


This is the histogram for the different prospective slopes we obtained, before we look for a particular line which has the best chi fit. We can see the slope mostly varies between -3 and 3 . Slope can atmost vary between -6 and 6

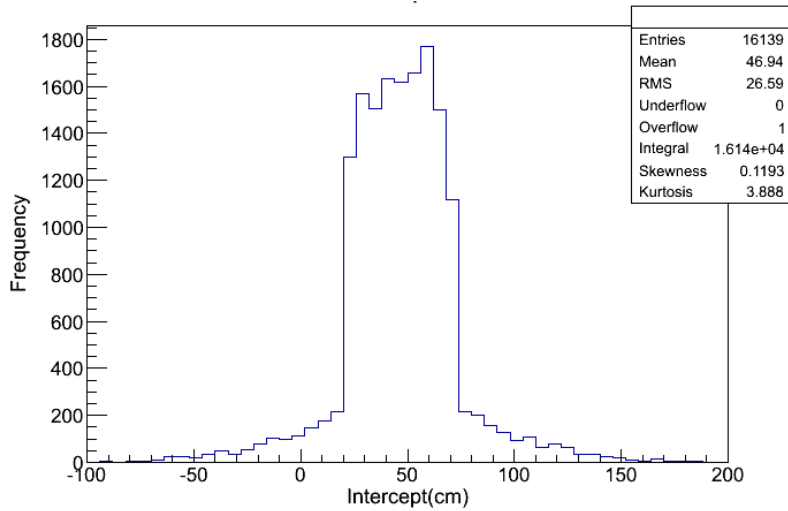


This is the histogram for the different intercept we obtained, before we look for a particular line which has the best chi fit.

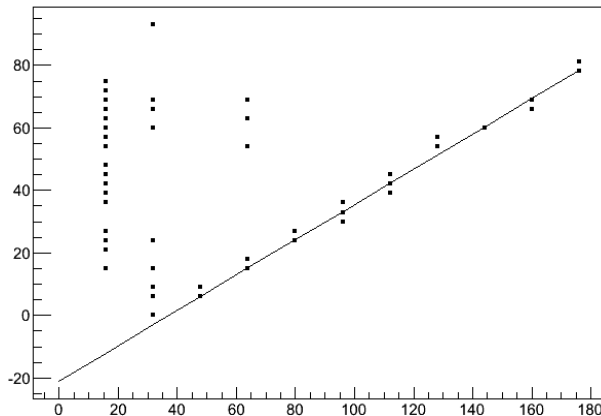
Plot for slopes and intercept obtained for the best chi line



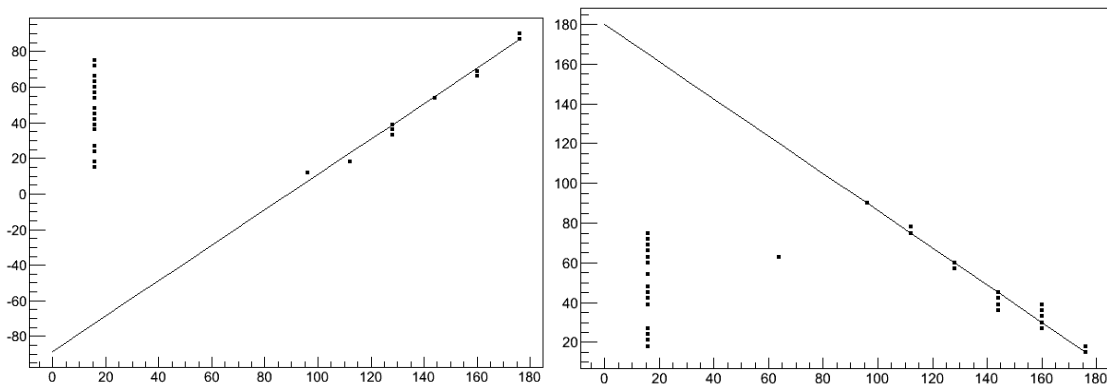
This is the histogram for the slopes we obtained for the best fitted muon tracks. We see that the range of slopes fitted varies from -0.5 to $+0.5$. This is In agreement with what we expect because the maximum possible slope = $32*3/12*16 = 0.5$



This is the histogram for the intercept we obtained for the best fitted muon tracks.

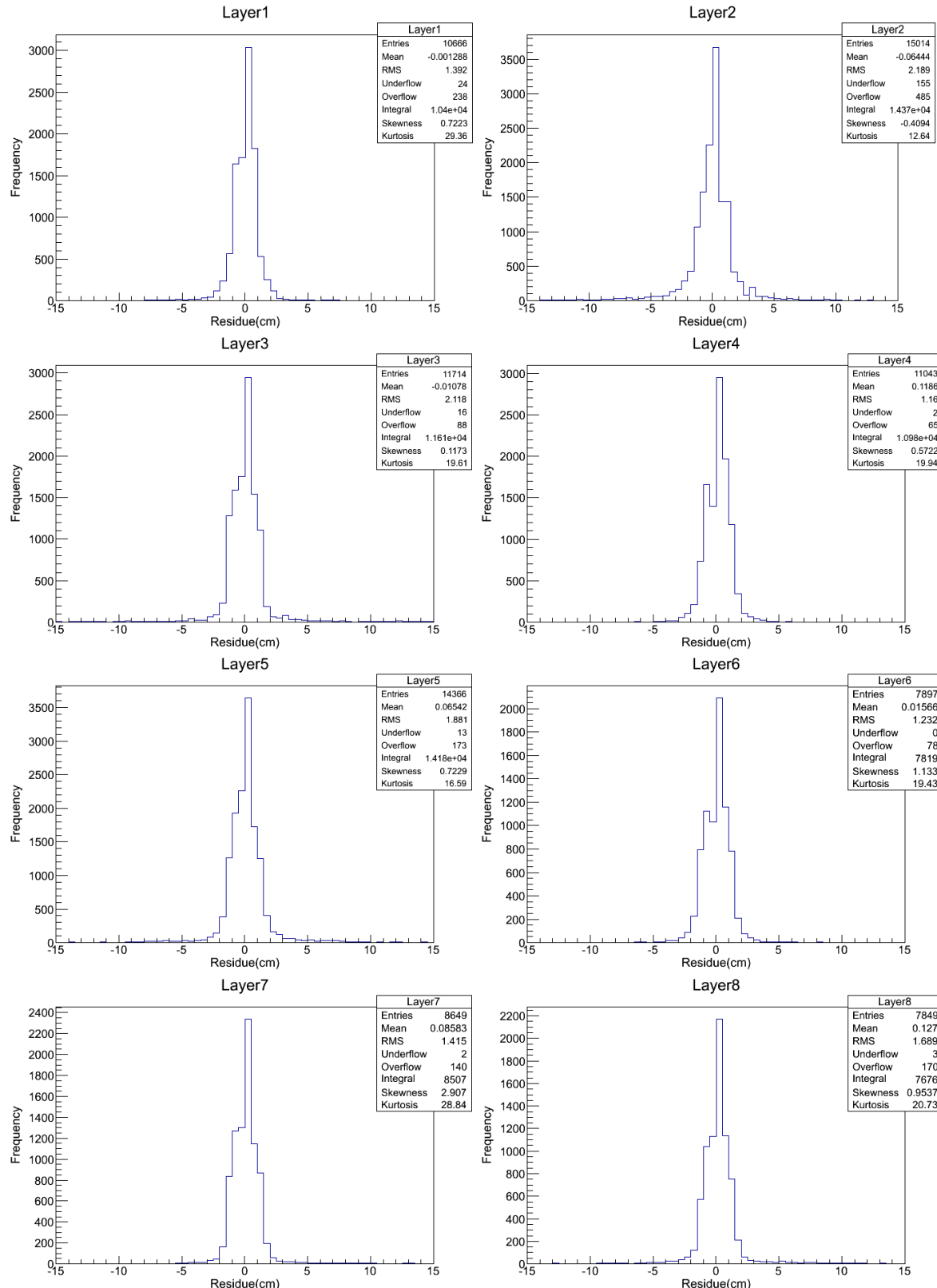


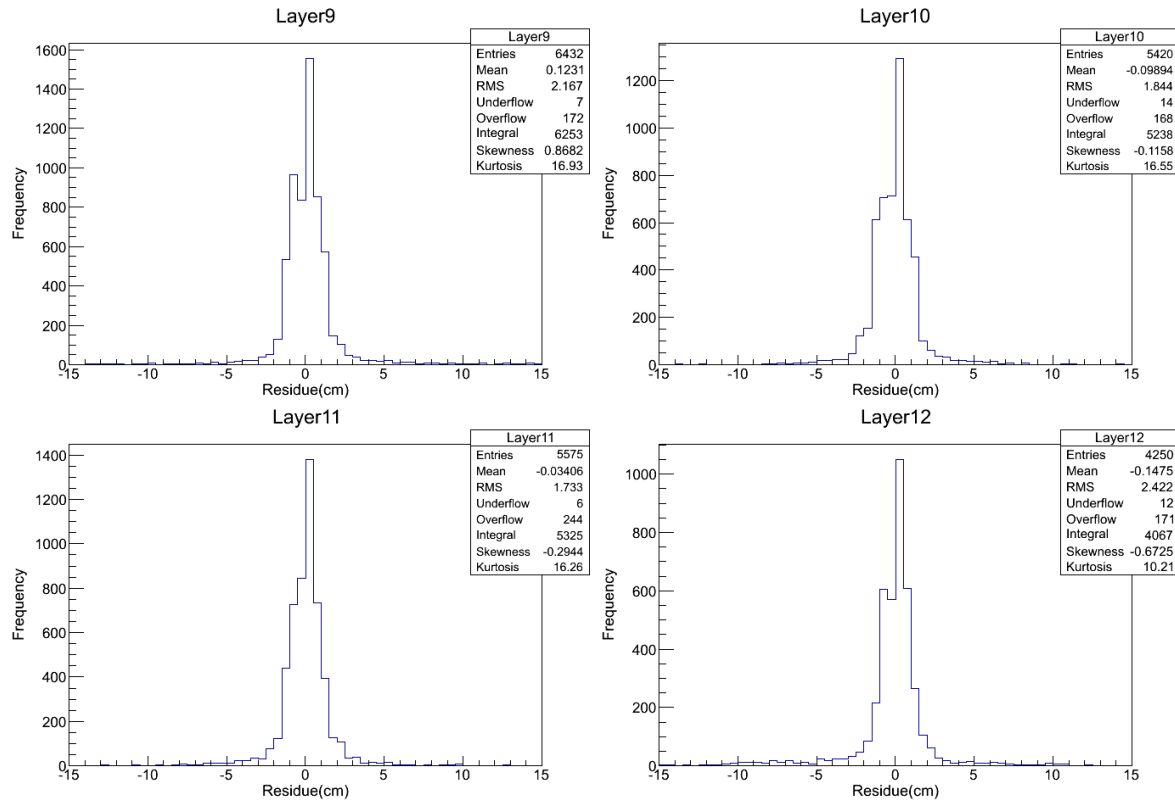
This is a track fit which shows that it is a good fit but still has a negative intercept.



These track fit show extreme values of intercept and still good fits. The presence of track only in the lower layers reflect that trigger came from a noisy layer and our data collected did not only capture vertical muons but also muons passing at large angles.

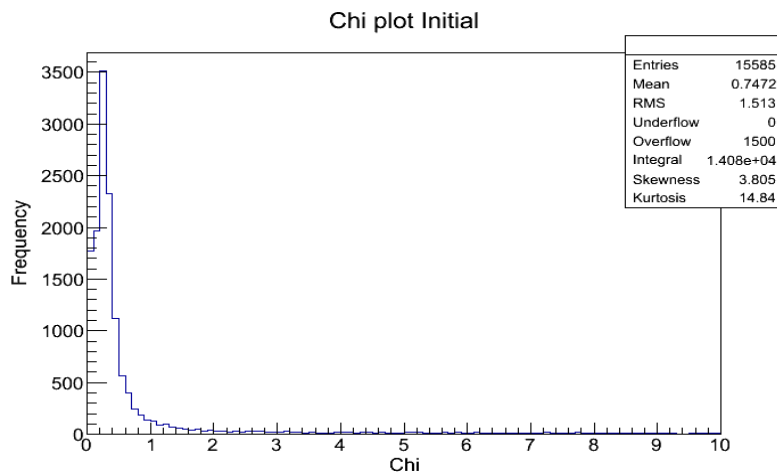
Plot for residue for layer 1-12





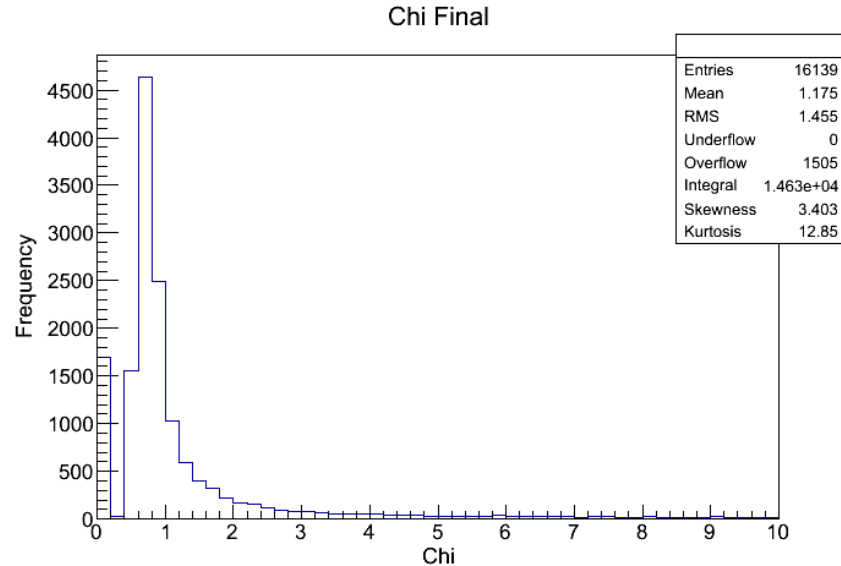
Residue varies mostly between -5cm and 5 cm and reflects that the fitted line is mostly within a distance of 1 strip from observed data

Plot for chi with atleast 4 layers with hits<=3



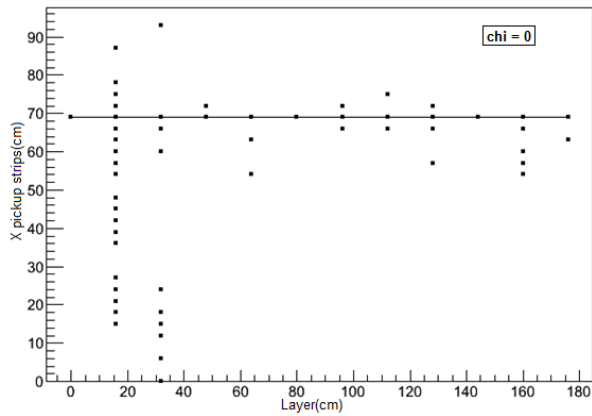
Initial Chi – fitted only 15585 events out of 21945. This algorithm took muon events for which atleast four layer with less than 3 hits were present. We further refined the algorithm to less than 5 hits and included more events.

Plot for chi with atleast 4 layers with hits<=5

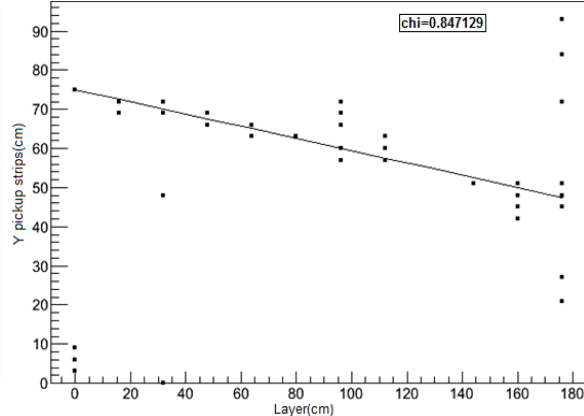


Final Chi – fitted only 16139 events out of 21945

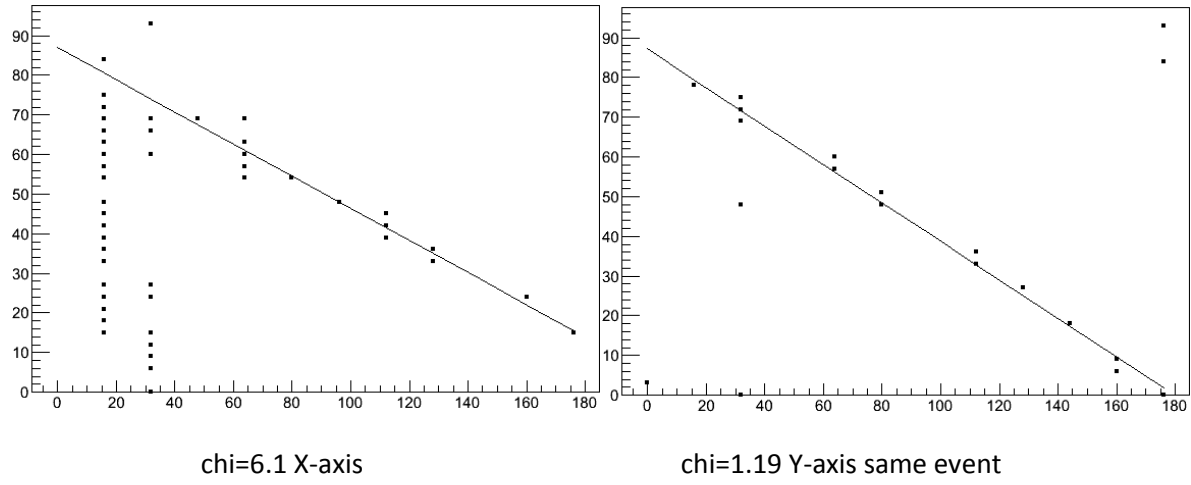
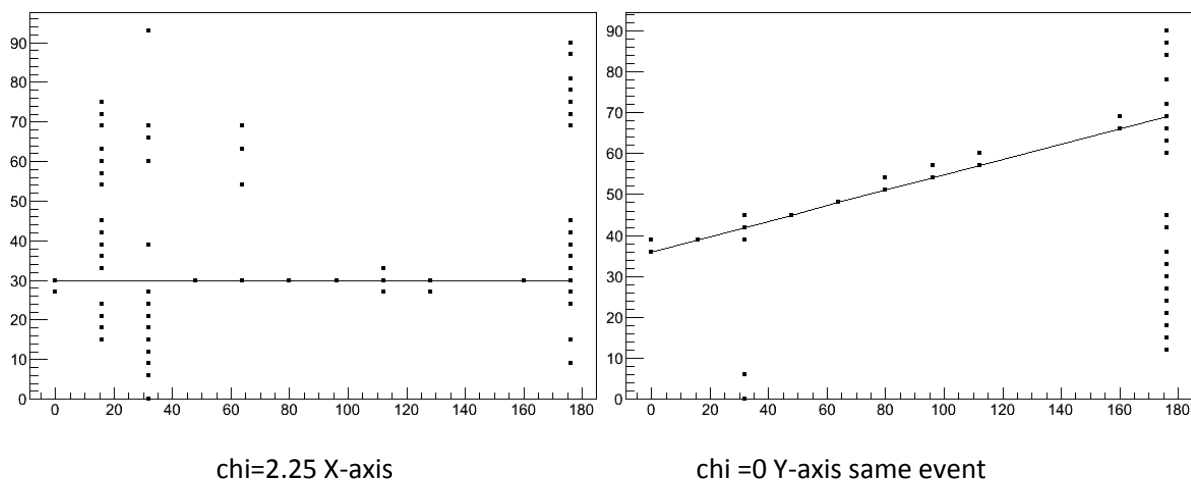
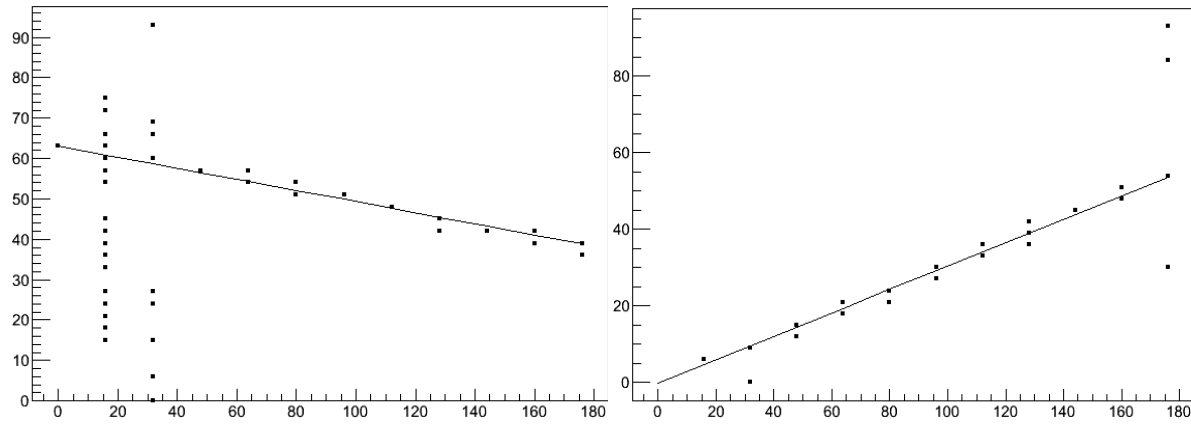
FITTED TRACKS

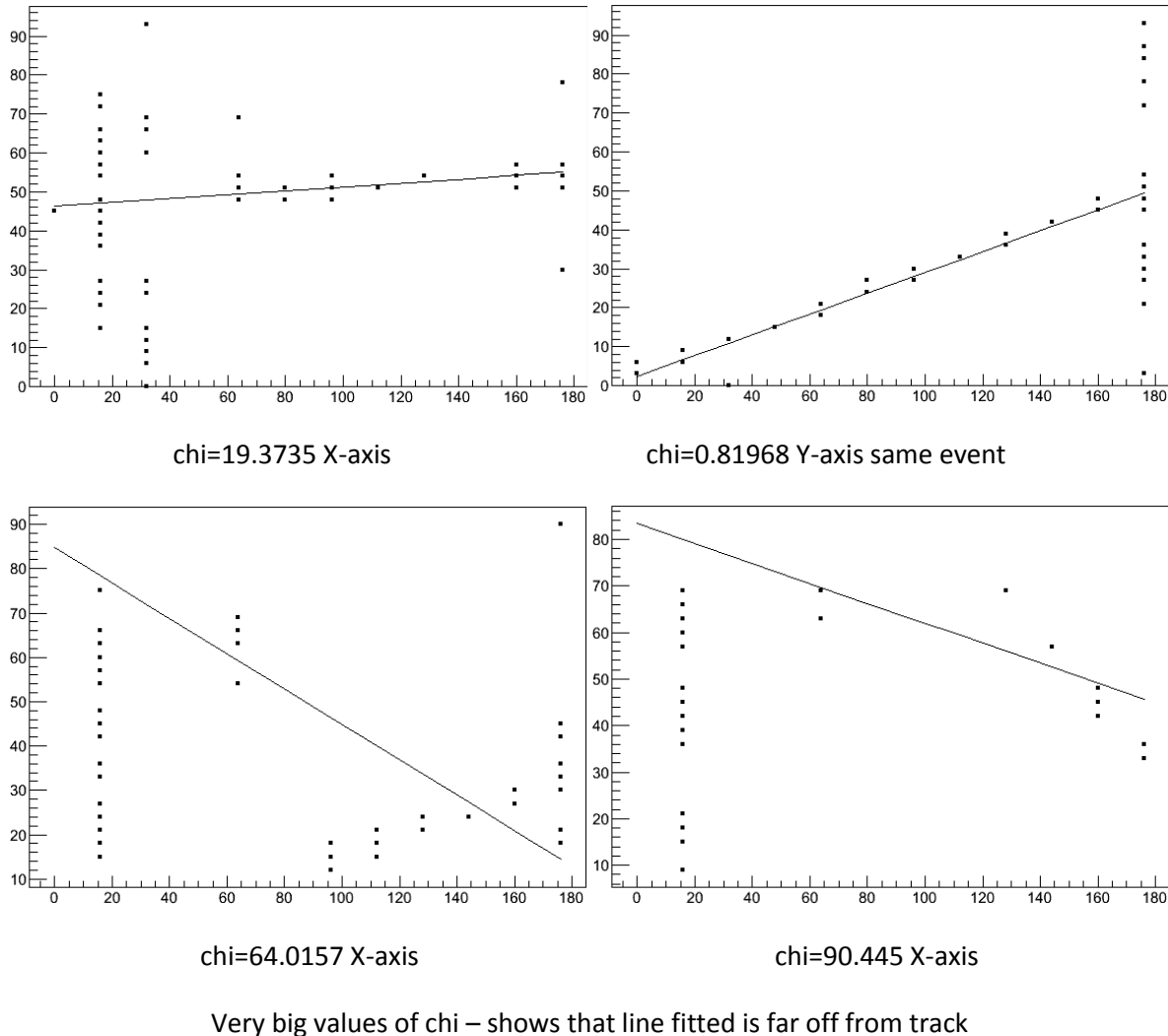


chi = 0 X-axis



chi = 0.847129 Y-axis same event

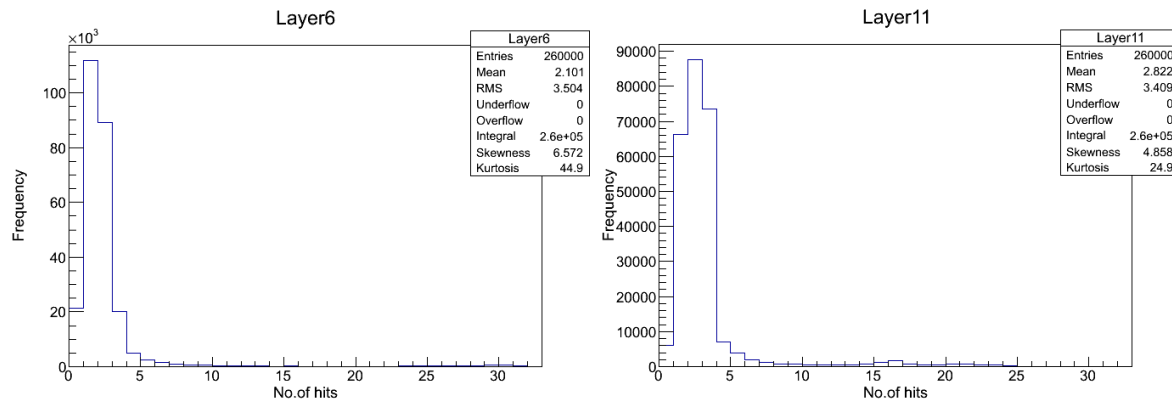




NOTE: The above data was taken on 17th May 2012. We conclude that out of 60000 events recorded only 21945 events showed muon tracks.

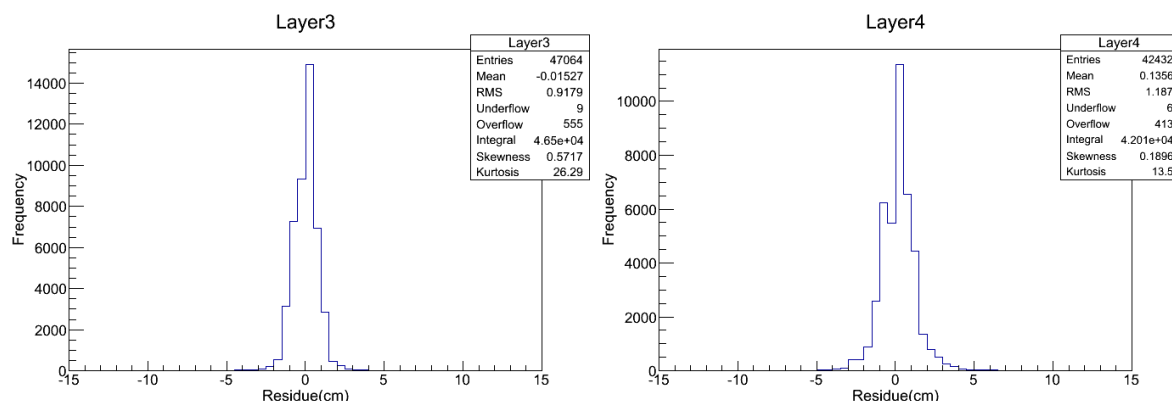
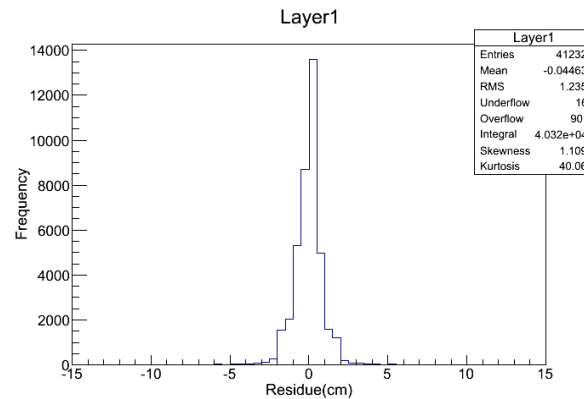
We again took data on 27th June, 2012. 2,60,000 events were recorded. 2,60,000 were analysed to look at the no. of hits in each layer. Only 68000 events were analysed for tracking and 65235 tracks were constructed as can be seen in the chi plot. We also plot residue plots for all the 12 layers for this data.

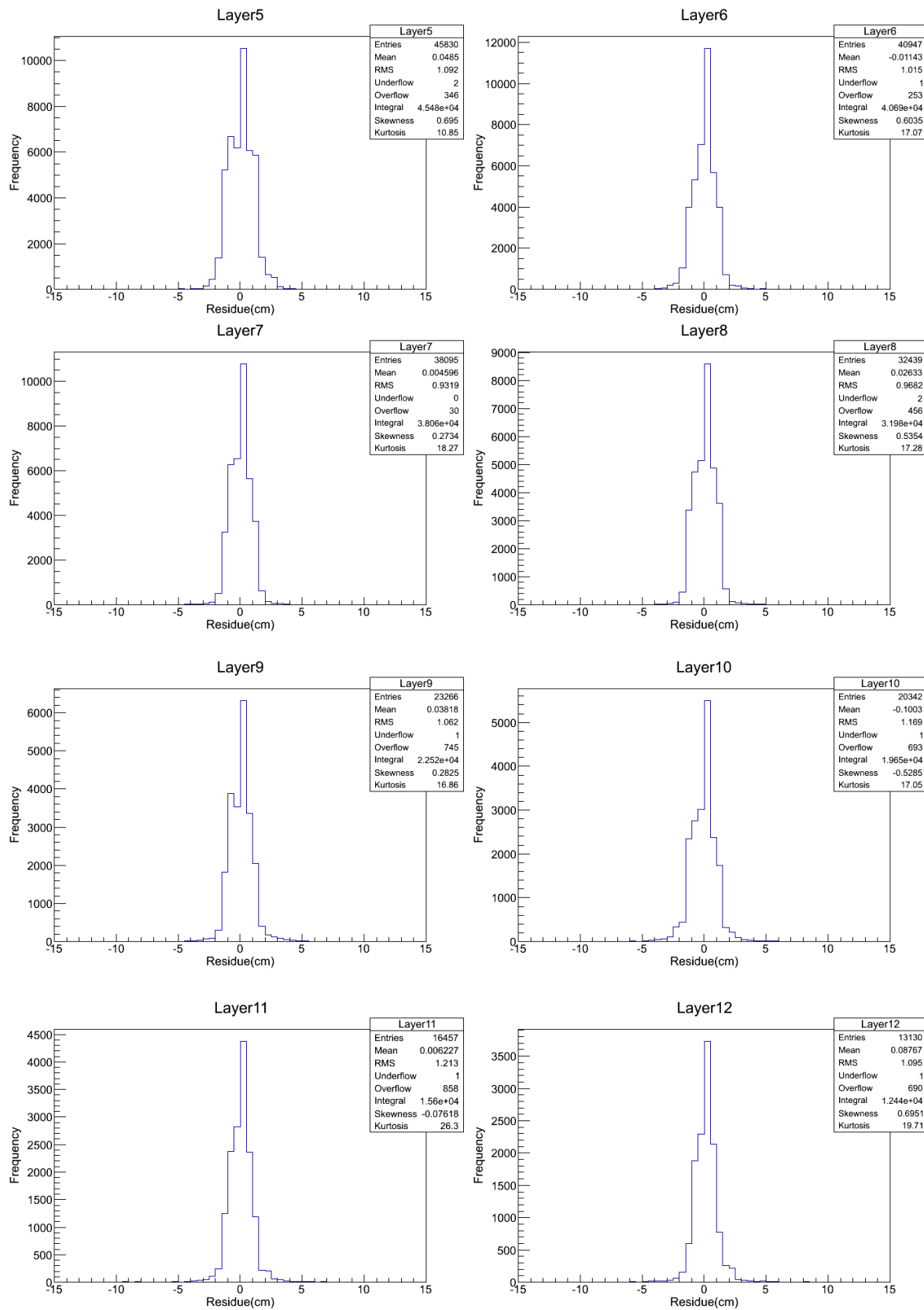
PLOTS FOR NO. OF HITS IN LAYER 6 AND LAYER 11 IS DISPLAYED

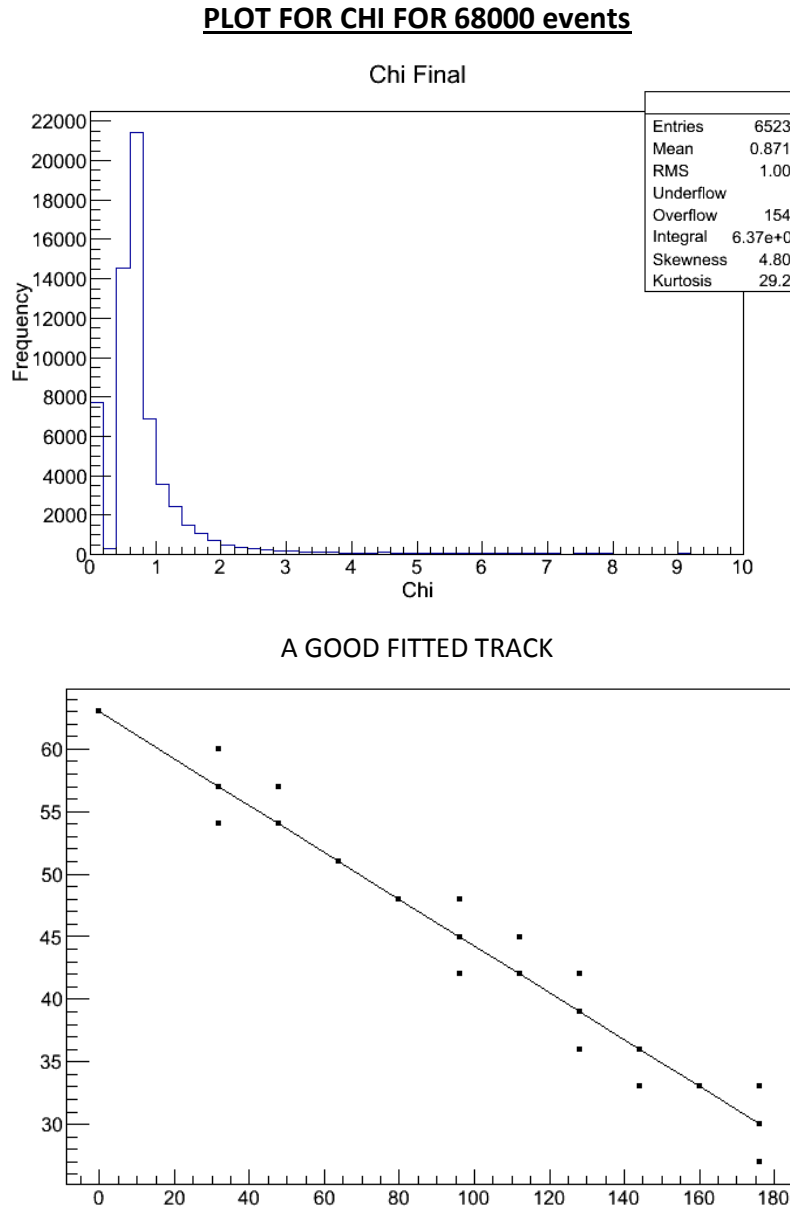


Layer 6 and 11 are typical layer with most events having mostly less than 5 hits

Plot for residue for layer 1-12







We further observe that most events lie in within the middle 12 strips. This is because our scintillator used for trigger was placed at the centre of the trigger layers and trigger was not produced if a muon passed at large angles or outside this region

APPENDIX:

NIM STANDARDS : The first standard established for nuclear and high energy Physics is a modular system called NIM (Nuclear Instruments Module). In this system, the basic electronic apparatus, for example, amplifiers, discriminators etc are constructed in the form of modules according to standard mechanical and electrical specifications. These modules, in turn, fit into NIM bins which supply them

with the standard power voltages. The co-axial cables used have a resistance of 50Ω . The voltage levels for logic 0 and logic 1 are 0V and -800mV respectively. 1m length of the cable causes a delay of 50ns.

DISCRIMINATORS: The discriminator is a device which responds only to input signals which have a pulse height above a certain threshold value (generally set such that the noise is eliminated). It acts basically as an analog-to-digital-converter. In an ADC, electronic signal is first used to charge a capacitor. The capacitor is then “run down”, i.e. discharged at a constant rate. At the start of the discharge, a scaler counting the pulses from a constant frequency clock or oscillator is gated on. When the capacitor has completely discharged, the scaler is gated off. The contents of the scaler is then a number proportional to the charge on the capacitor.

There are two kinds of discriminators used

Leading Edge Discriminator: The logic signal is generated at the moment the analog pulse crosses the threshold. This method is inherently subject to the problem of “walk” but can be used with good results if the amplitudes are restricted to a small range.

Constant Fraction Discriminators: The logic signal is generated at a constant fraction of the peak height to produce an essentially walk-free timing signal. Depending on the type of signal, this level occurs at a constant fraction of the pulse independent of its amplitude.

Walk and Jitters : The most important factor in any timing system is its resolution. One method to measure the resolution is to measure the time difference of two exactly coincident signals.

The *walk* effect is caused by variations in the amplitude and/or risetime of the incoming signals. Imagine two signals of differing pulse height but exactly coincident in time. Due to the difference in pulse height, the two signals will trigger the discriminator at different times even though they are exactly coincident. This dependence on amplitude causes the signal to *walk* about. A second source of *walk*, although much smaller in effect, is the finite amount of charge necessary to trigger the discriminator. In general, after reaching the discriminator threshold, a certain amount of charge must be integrated on a capacitor before a logic signal is emitted.

Timing fluctuations are also caused by noise and statistical fluctuations in the original detector signal. Because of these random fluctuations, two identical signals will not always trigger at the same point, giving instead a time variation dependent on the amplitude of fluctuations. This effect is usually referred to as *time jitter*.

ANALOG TO DIGITAL CONVERTER : The input signal is first used to charge a capacitor. The capacitor is then “run down” i.e. discharged at a constant rate. At the start of the discharge, a scaler counting the pulses forms a constant frequency clock or oscillator is gated on. When the capacitor has completely discharged, the scaler is gated off. The contents of the scaler is then a number proportional to the charge on the capacitor.

ACKNOWLEDGEMENTS:

I am greatly indebted to my project advisor, Professor Sudeshna Banerjee for guiding me at each step. I am also thankful to Mr. L V Reddy, R. R. Shinde, Sumanta Pal, Sudeshna Dasgupta and all the members of the lab.

REFERENCES :

- [1] B. Satyanarayan, "Design and Characterisation Studies of Resistive Plate Chamber ", TIFR, 2009